

Supplementary Information

One-Pot Synthesis of Anatase, Rutile Decorated Hydrogen Titanate Nanorods by Yttrium Doping for Solar H₂ Production

Sovann Khan^a, Hiroshi Ikari^a, Norihiro Suzuki^{a,b}, Kazuya Nakata^{a,c}, Chiaki Terashima^{a,b}, Akira Fujishima^a, Ken-ichi Katsumata^{a,b,d*} and Vicente Rodríguez-González^{a,e*}

^aPhotocatalysis International Research Center, Tokyo University of Science, 2641 Yamazaki, Noda-shi, Chiba 278-8510, JAPAN

^bResearch Center for Space Colony, Tokyo University of Science, 2641 Yamazaki, Noda-shi, Chiba 278-8510, JAPAN

^cGraduate School of Bio-Applications and Systems Engineering, Tokyo University of Agriculture and Technology, 2-24-16 Nakacho, Koganei, Tokyo 184-0012, JAPAN

^dDepartment of Materials Science and Technology, Faculty of Industrial Science and Technology, Tokyo University of Science, 6-3-1 Niijuku, Katsushika-ku, Tokyo 125-8585, JAPAN

^eInstituto Potosino de Investigación Científica y Tecnológica (IPICYT), División de Materiales Avanzados, Camino a la Presa San José 2055, Lomas 4a. sección 78216, San Luis Potosí, Mexico

*Corresponding to:

(K. Katsumata) k.katsumata@rs.tus.ac.jp and

(V. Rodríguez-González) vicente.rdz@ipicyt.edu.mx

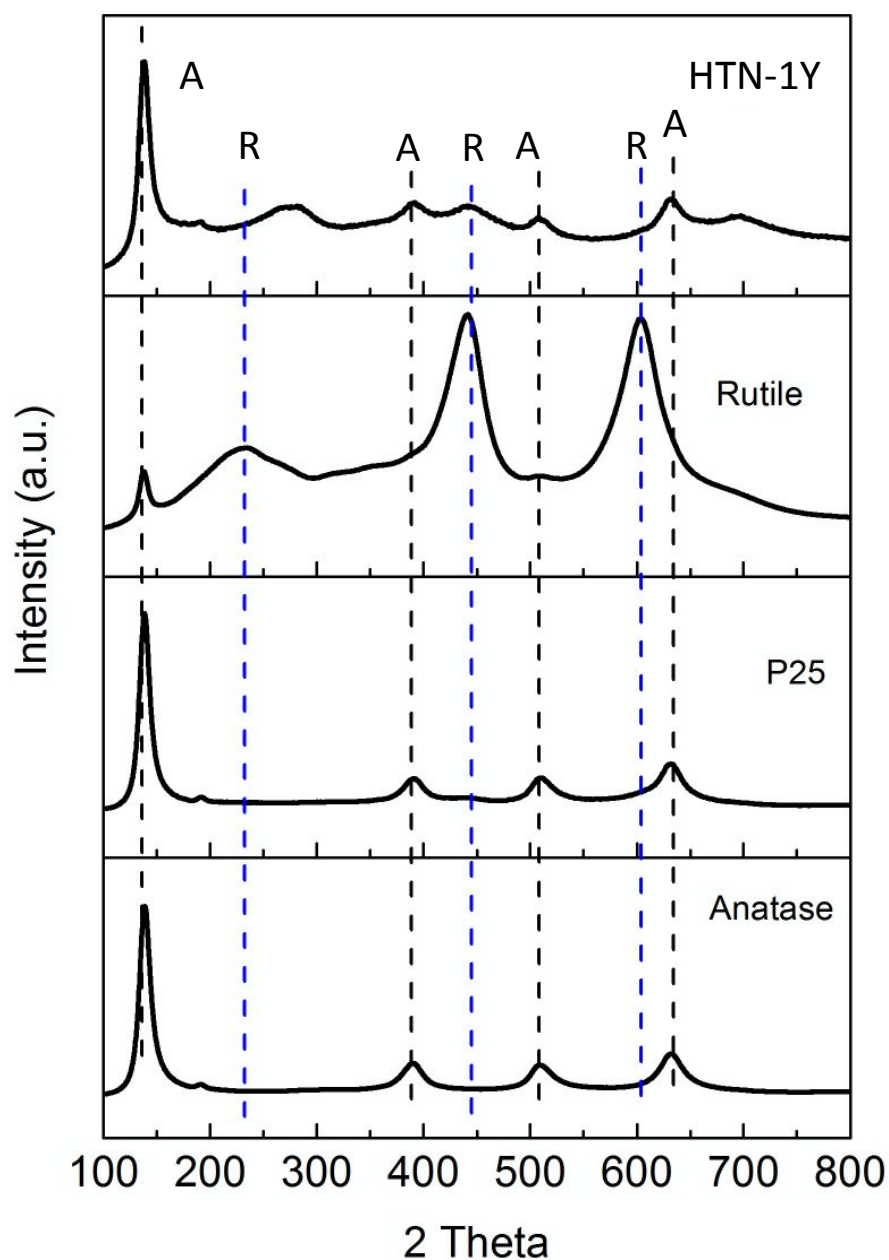


Figure S1: Comparing Raman spectra of anatase, P25, rutile and HTN-1Y
 [Anatase and rutile were synthesized by solvothermal method followed by 2 h-450 °C-
 annealing for anatase and 5 h-850 °C-annealing for rutile]

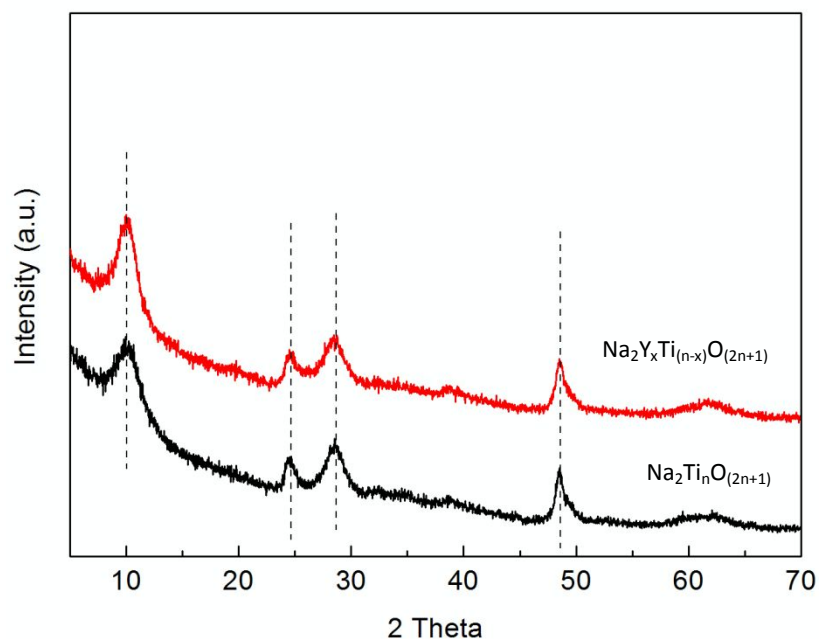


Figure S2: XRD spectra of sodium titanate and Y-doped sodium titanate: Due to the broad peaks of XRD peaks, multiple phases of sodium titanates were fitted including major phases of $\text{Na}_2\text{Ti}_3\text{O}_7$ (JCPDS#31-1321), $\text{Na}_2\text{Ti}_4\text{O}_9$ (JCPDS#33-1294) and $\text{Na}_2\text{Ti}_6\text{O}_{13}$ (JCPDS#37-0951). So, we represented $\text{Na}_2\text{Ti}_n\text{O}_{(2n+1)}$ as produced titanates and $\text{Na}_2\text{Y}_x\text{Ti}_{(n-x)}\text{O}_{(2n+1)}$ as Y-doped titanate. Although the peaks were identical between Y-doped and undoped sample, small shift to lower angles was observed, which should be due to the increase of crystal cells by Y-doping.

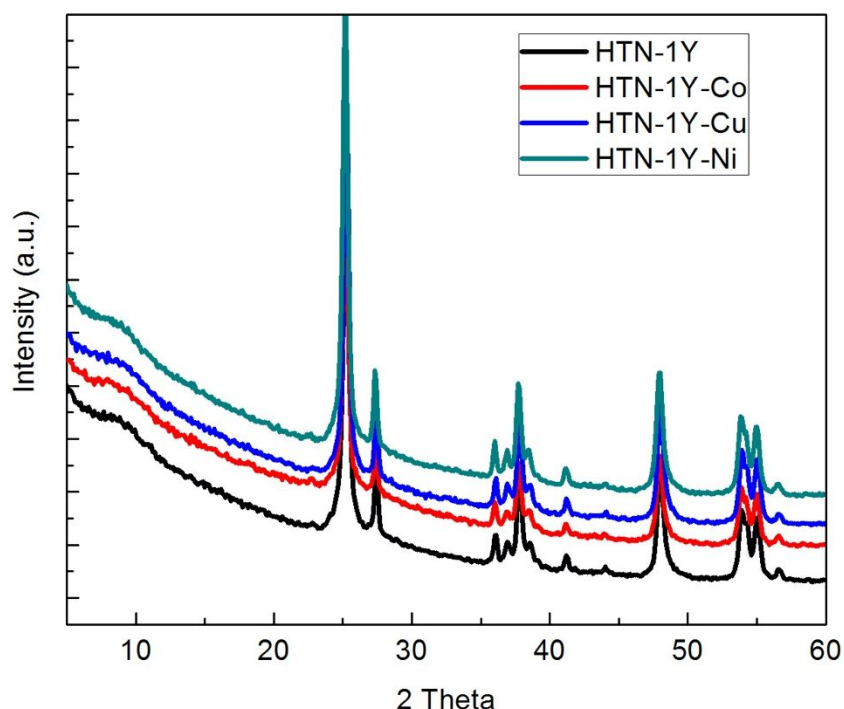


Figure S3: XRD spectra of HTN-1Y and HTN-1Y loading with Co, Cu and Ni [There was no important change with metal loading. No metal peaks were observed. This might due to the low concentration of metal loading]

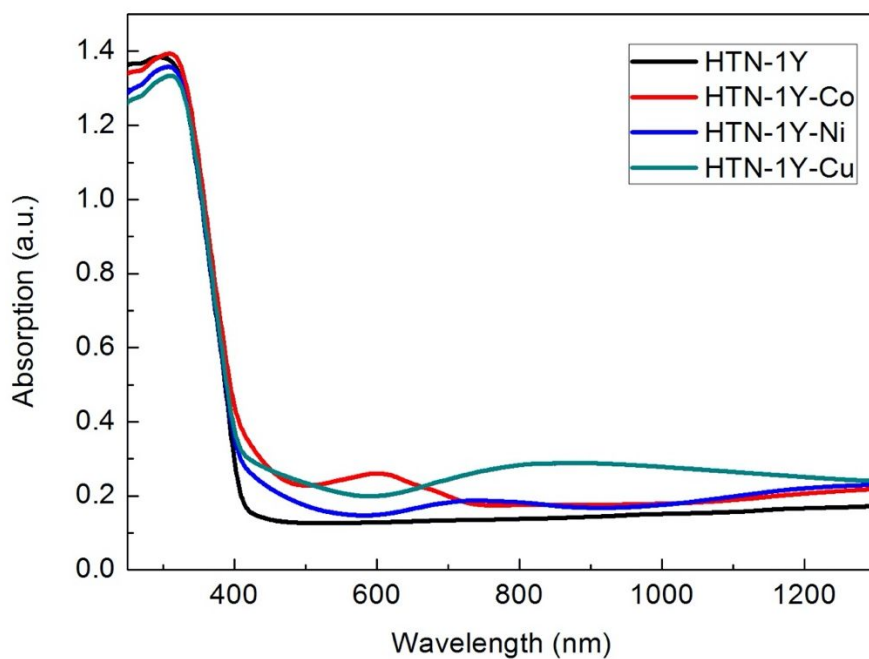


Figure S4: UV-vi-NIR absorption spectra of HTN-1Y and loaded samples with Co, Ni and Cu

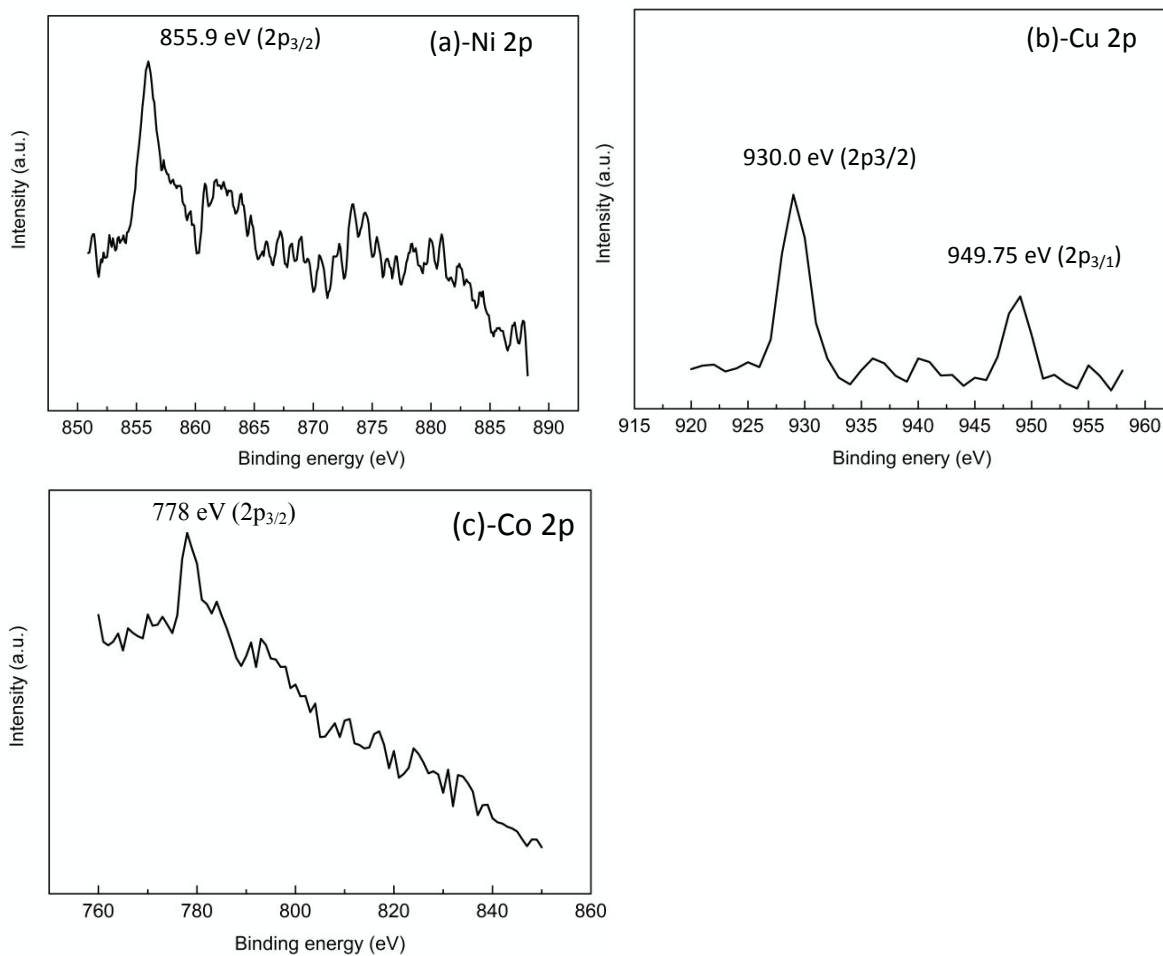


Figure S5: XPS spectra of (a) Ni 2p, (b) Cu 2p and (c) Co 2p from for metal-loaded HTN-Y samples

XPS of Ni 2p: Intense peak at ~ 855.9 eV was known as binding energy of Ni^{2+} (inform of NiO or Ni(OH)_2) [1]. No Ni^0 specie was observed (~ 582.1 eV [2]). XPS of Cu 2p: The observed peaks of binding energies were at 930.0 eV and 949.75 ($\Delta E \sim 18.75$), which were identified as spin-orbit splitting components of $2p_{3/2}$ and $2p_{1/2}$ [3,4]. The absence of satellite peaks at around ~ 943 eV confirmed that no Cu^{2+} species was presented in our samples, which inferred the complete reduction of Cu^{2+} precursor to Cu^0 metal by ZnS-ZnO photoreduction [3-5]. XPS of Co 2p: The intense peak at 778 eV was attributed to $2p_{3/2}$ of Co^0 . Other oxidative states of Co such as Co^{2+} (inform of CoO , or Co(OH)_2) and Co^{4+} (inform of Co_3O_4), which were observed at binding energies greater than 780 eV [5], were not found in our sample. Therefore, Co metal should be the major phase in our loading sample. The concentrations of Ni, Cu and Co calculated from XPS spectra were 1.45 at.%, 0.35 at.% and 0.55 at.%, respectively.

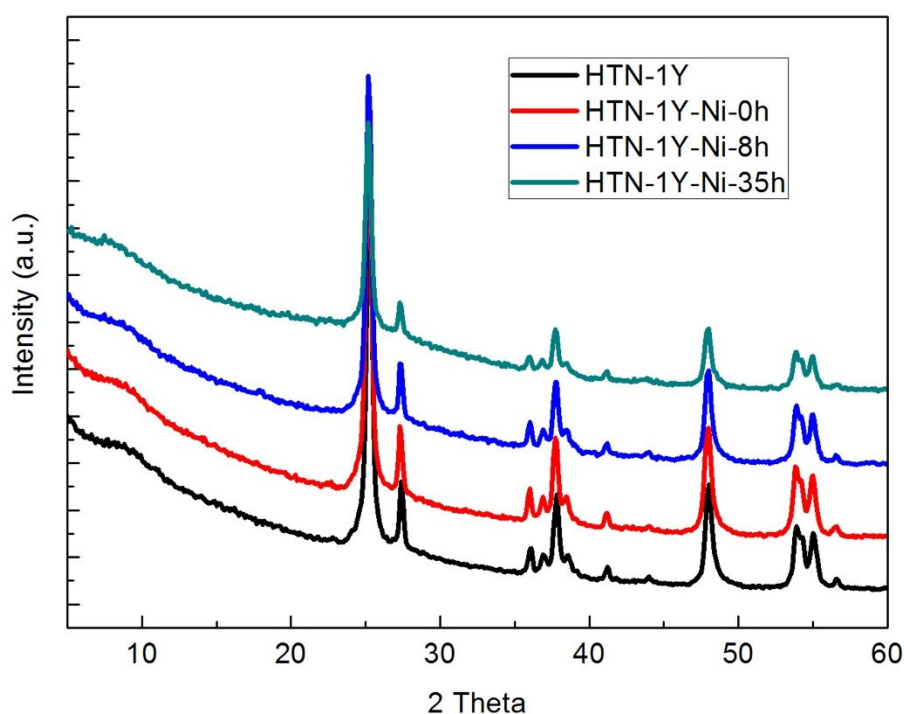


Figure S6: XRD spectra of HTN-Y and HTN-Y loading with Ni before and after 8h and 40 h reaction

[Phases were maintained after 35 reaction, however lower XRD peak inferred the low crystallinity. This might be due to corrosion of particles under UV radiation.]

Comparing with other works:

We have selected several related works on titanates and loading photocatalyst for comparing with our work. Ide et al. (2018) induced anatase phase deposited on the $\text{K}_2\text{Ti}_4\text{O}_9$ by chemical dissolution and recrystallization under hydrothermal treatment [7]. H_2 generation by Ni-loaded $\text{K}_2\text{Ti}_4\text{O}_9$ /anatase catalyst was very low under visible light (> 450 nm). Quantum yield (QE) was 0.0002%. In similar process from the same group, Esmat et al. (2019) produced 2D structures of layered $\text{K}_x\text{Ti}_{2-x/3}\text{Li}_{x/3}\text{O}_4$ /anatase and tested photocatalytic activities for H_2 evolution under solar simulator [8]. H_2 production rate was 0.3 mmol/g/h, which was lower than that of our samples although they used precious Pt metal as cocatalyst. By assuming UV fraction in 1 sun is $\sim 5\%$. Therefore, UV light intensity in their work is ~ 5 mW/ cm^2 , which was still stronger than our light intensity. Our samples' performances were much better. Saito et al. (2017) prepared $\text{H}_{1.07}\text{Ti}_{1.73}\text{Li}_{0.27}\text{O}_4$ /rutile heterostructure by treated $\text{K}_{0.8}\text{Ti}_{1.73}\text{Li}_{0.27}\text{O}_4$ with diluted HCl and dried under room temperature under reduced pressure [9]. H_2 production rate

under solar simulator with Pt-loading showed higher than that of our samples (HTN-1Y) loading with Ni and Co. But, this rate is less than that of Cu-loaded HTN-1Y. Another interesting work on mixed $H_{1.07}Ti_{1.73}\square_{0.27}O_4$ and P25 done by Saito et al. (2016) showed very high quantum yield (23% at 320 nm) [10]. My mixing with P25, H_2 production rate from ethanol-water solution under solar simulator was increased by 6 times, compared to pure $H_{1.07}Ti_{1.73}\square_{0.27}O_4$. $H_{1.07}Ti_{1.73}\square_{0.27}O_4$ /P25 in this work shows much higher than that our sample. This might be due to synergetic effects of highly active P25 and $H_{1.07}Ti_{1.73}\square_{0.27}O_4$. Another similar work on nickel intercalated into titanate nanotube was reported by Jang et al. (2011) [11]. H_2 production under Hg-lamp was improved by 3.5 times with nickel intercalating. However, their H_2 production rate so much lower than our samples.

In summary, HTN-Y in this work showed comparable or even better performance on photocatalytic H_2 generation compared to other titanate catalysts (Ni-intercalated $Na_2Ti_2O_5 \cdot nH_2O$, $K_2Ti_4O_9$ /anatase, $K_xTi_{2-x/3}Li_{x/3}O_4$ /anatase). However, HTN-Y still showed less activities than commercial P25.

Table S1: Comparison of recent works

Materials	Solution	Lamp	Catalyst loading (mg/mL)	Surface area (m ² /g)	Production rate * (mmol/g/h)	QE (%)	Ref.
HTN				300	0.009	-	
HTN-1Y				165	<u>0.072</u>	-	
Ni-HTN-Y	Methanol-water	UV (2.4 mW/Cm ²)	50/50	-	<u>6.668</u>	0.43 [365nm]	This work
Co-HTN-1Y				-	5.289	0.18 [365nm]	
Cu-HTN-1Y				-	11.683	2.25 [365nm]	
Ni-P25				44.8	<u>8.97</u>	-	
Ni-HTN-1Y	Methanol-water	Visible (4.7 mW/Cm ²)-400nm-cutt-off	50/50	-	<u>0.049</u>	-	This work
Co-HTN-1Y				-	<u>0.011</u>	-	
Cu-HTN-1Y				-	<u>0.279</u>	-	
Ni-P25				-	<u>0.007</u>	-	
Ni-K ₂ Ti ₄ O ₉ /Anatase	Methanol-water	150 W-Xe lam (450 nm-cutt)	15/5	-	0.005x10 ⁻³	0.0002 [450 nm]	2018 [7]
Pt-K _x Ti _{2-x/3} Li _{x/3} O ₄ /Anatase	Methanol-water	Solar simulator (1000 W/m ²)	15/5	-	~0.30	-	2019 [8]
Pt-H _{1.07} Ti _{1.73} □ _{0.27} O ₄ /Rutile	Methanol-water	Solar simulator (1000 W/m ²)	15/5	51	~8.22	14.1 [320 nm]	2017 [9]
H _{1.07} Ti _{1.73} □ _{0.27} O ₄ /P25	Methanol-water	Solar simulator (1000 W/m ²)	15/5	-	~0.67	23 [320 nm]	2016 [10]
Ni-Na ₂ Ti ₂ O ₅ ·nH ₂ O	Methanol-water	Hg-arc (450W)	100/100	-	~0.90	-	2009 [11]

*Different works reported unit of H_2 production rates. For comparing, production rates were assumed based on average H_2 production per hour divided by catalyst used.

Reference:

1. Natascha Weidler, Jona Schuch, Florian Knaus, Patrick Stenner, Sascha Hoch, Artjom Maljusch, Rolf Schafer, Bernhard Kaiser, and Wolfram Jaegermann, X-ray photoelectron spectroscopic investigation of plasma-enhanced chemical vapor deposited NiO_x , $\text{NiO}_x(\text{OH})_y$, and $\text{CoNiO}_x(\text{OH})_y$: Influence of the chemical composition on the catalytic activity for the oxygen evolution reaction, *J. Phys. Chem. C* **2017**, *121*, 6455–6463.
2. Amol M. Hengne, Akshaya K. Samal, Linga Reddy Enakonda, Moussab Harb, Lieven E. Gevers, Dalaver H. Anjum, Mohamed N. Hedhili, Youssef Saih, Kuo-Wei Huang and Jean-Marie Basset, Ni–Sn-supported ZrO_2 catalysts modified by indium for selective CO_2 hydrogenation to methanol, *ACS Omega* **2018**, *3*, 3688–3701.
3. Jian Sun, Jianfeng Yu, Qingxiang Ma, Fanquiong Meng, Xiaoxuan Wei, Yannan Sun, Noritatsu Tsubaki, Freezing copper as noble metal-like catalyst for preliminary hydrogenation, *Sci. Adv.* **2018**, *4*, eaau3275:1–10
4. Bo-Ren Chen, Van-Huy Nguyen, Jeffrey C.S. Wu, Reli Martin and Kamila Koci, Production of renewable fuels by the photohydrogenation of CO_2 : Effect of the Cu species loaded onto TiO_2 photocatalysts, *Phys. Chem. Chem. Phys.* **2016**, *18*, 49424951.
5. Meenakshi Chauhan, Kasala Prabhakar Reddy, Chinnakonda S. Gopinath and Sasanka Deka, Copper cobalt sulfide nanosheets realizing a promising electrocatalytic oxygen evolution reaction, *ACS Catal.* **2017**, *7*, 5871–5879.
6. Alexander A. Khassin, Tamaraa M. Yurieva, Vasiliy V. Kaichev, Valerii I. Bukhatiyarov, Anna A. Budneva, Evgeniy A. Paukshitis, Valentin N. Parmon, Metal-support interactions in cobalt-aluminum co-precipitated catalysts: XPS and CO adsorption studies, *J. Mol. Catal. A: Chem.* **2001**, *175*, 189–204.
7. Yusuke Ide, Wataru Shirae, Toshiaki Takei, Durai Mani, and Joel Henzie, Merging Cation Exchange and Photocatalytic Charge Separation Efficiency in an Anatase/ $\text{K}_2\text{Ti}_4\text{O}_9$ Nanobelt Heterostructure for Metal Ions Fixation, *Inorg. Chem.* **2018**, *57*, 6045–6050.
8. Mohamed Esmat, Ahmed A. Farghali, Samaa. I. El-Dek, Mohamed H. Khedr, Yusuke Yamauchi, Yoshio Bando, Naoki Fukata, and Yusuke Ide, Conversion of a 2D Lepidocrocite-Type Layered Titanate into Its 1D Nanowire Form with Enhancement of Cation Exchange and Photocatalytic Performance, *Inorg. Chem.* **2019**, *58*, 7889–7996.
9. Kanji Saito, Satoshi Tominaka, Shun Yoshihara, Koji Ohara, Yoshiyuki Sugahara, and Yusuke Ide, Room-temperature rutile TiO_2 nanoparticle formation on protonated layered titanate for high-performance heterojunction creation, *ACS Appl. Mater. Interfaces* **2017**, *9*, 24538–24544.
10. Kanji Saito, Misa Kozeni, Minoru Sohmiya, Kenji Komaguchi, Makoto Ogawa, Yoshiyuki Sugahara and Yusuke Ide, Unprecedentedly enhanced solar photocatalytic activity of a layered titanate simply integrated with TiO_2 nanoparticles, *Phys. Chem. Chem. Phys.* **2016**, *18*, 30920–30925
11. Jum Suk Jang, Sun Hee Choi, Dong Hyun Kim, Ji Wook Jang, Kyung Sub Lee, and Jae Sung Lee, Enhanced photocatalytic hydrogen production from water-methanol solution by nickel intercalated into titanate nanotube, *J. Phys. Chem. C*, **2009**, *113*, 8990–8996.